

Application Note #150

Characterization of Advanced Semiconductor Materials and Processes with Nanoscale IR Spectroscopy

Submicron and nanoscale chemical identification of semiconductor materials, specifically those that are organic, is a significant challenge in the research of devices, as well as in process control and failure analysis environments. Because of this, there are a multitude of techniques used by semiconductor manufacturers to identify chemical components.

Scanning electron microscopy coupled with energy dispersive X-ray spectroscopy (SEM/EDX) is the industry standard in surface analysis, and offers nanometer-scale spatial resolution with semi-quantitative elemental analysis. While this elemental analysis offers useful chemical insight into surface defects and contaminations, it is fairly limited in identifying organic materials.

Infrared (IR) spectroscopy is a powerful technique for chemical characterization of organic species that cannot be readily identified by SEM/EDX. However, traditional IR spectroscopic techniques are limited by Abbe diffraction laws to spatial resolutions between 3–10 μm , depending on the technique used.

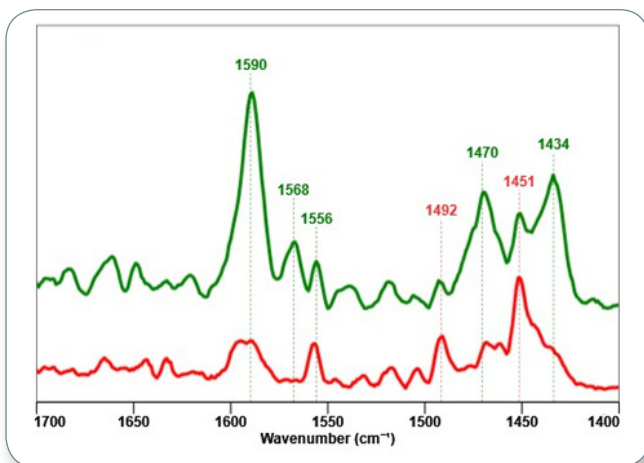
Atomic force microscopy (AFM) is a widely used nanoscale imaging technique which provides the user with a high spatial resolution topographic map of a sample surface. Until now, the major drawback of AFM has been its inability to chemically characterize the material underneath the tip.

Resonance-Enhanced AFM-IR and Tapping AFM-IR

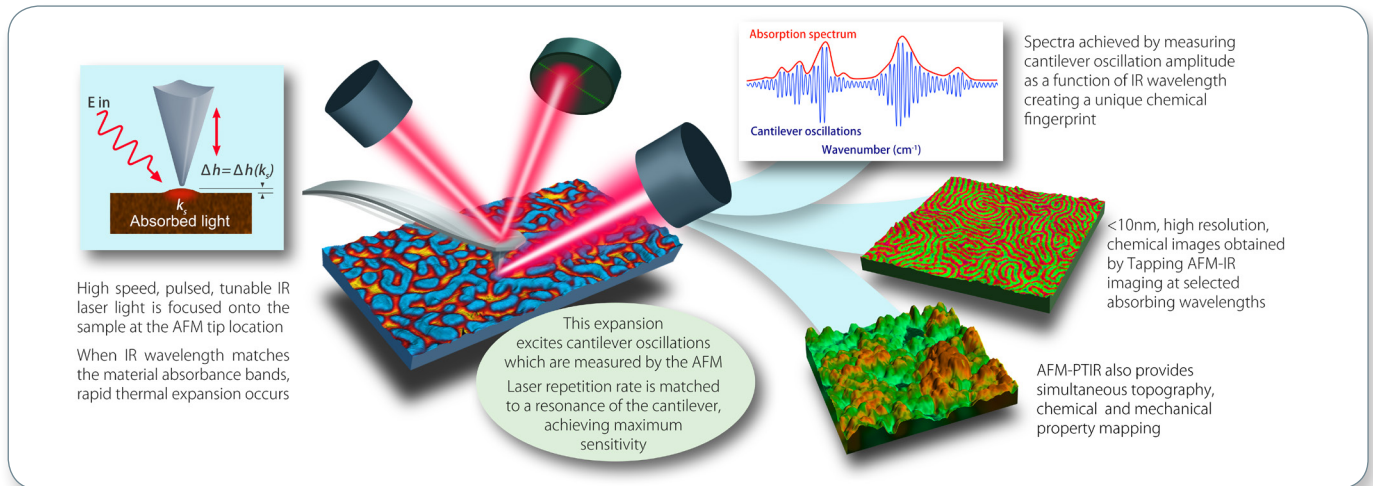
Nanoscale IR spectroscopy overcomes these limitations by combining AFM and IR techniques to achieve nanoscale FTIR spectroscopy using photothermal IR spectroscopy (PTIR). Nanoscale IR spectroscopy combines the precise chemical identification of IR spectroscopy with the nanoscale capabilities of AFM to chemically identify sample components with a spatial resolution below 10 nm and with monolayer sensitivity, breaking the diffraction limit by >100x. AFM-PTIR absorption spectra are direct measurements of sample absorption, independent of other complex optical properties of the tip and sample. As such, AFM-PTIR spectra correlate well to conventional bulk IR spectra.¹

Nanoscale Organic Contaminants

To demonstrate nanoscale chemical characterization capabilities on the nanoIR3, contaminated silicon wafers were first prepared using known materials typical of those found in semiconductor fabrication environments, and then analyzed. For each sample, high-resolution tapping mode



Tapping AFM-IR spectra clearly identifying each chemical component of a block copolymer material.



AFM images were acquired to locate the contaminants, followed by respective nanoIR measurements.

The AFM height image shown in Figure 1a illustrates the thickness variation (20-100 nm) of the contaminant residue (human skin tissue) on the wafer. After locating a point of interest in the AFM image, the probe is positioned in the desired location, and the laser wavelength is scanned to acquire the nanoIR spectra, as seen in Figure 1b. Spectra were then collected at sites with varied sample thickness. As expected, the observed IR intensities differed with sample thickness; however, the overall signal-to-noise ratio is sufficient to accurately identify the material, even at 20 nm thickness, reflecting the excellent sensitivity in detection of thin samples.

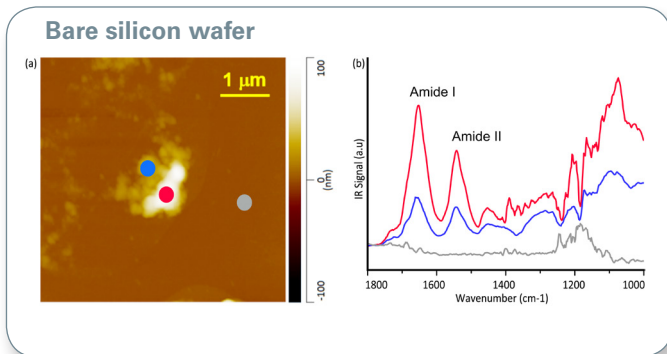


Figure 1. AFM height image (a) and corresponding AFM-IR spectra (b) of organic residue on a silicon wafer show clear Amide I and II bands, indicating human skin residue. The colored line spectra corresponded to colored measurement pixels in the AFM image.

New FASTspectra capabilities on the nanoIR3 enable faster acquisition of spectra over the full IR tuning range, allowing for a reduction in spectral acquisition time by a factor of 10. This is accomplished by the laser source sweeping over its range, while the cantilever oscillation amplitude is measured simultaneously with the wavelength change, illustrated in Figure 2.

To demonstrate the correlation to conventional FTIR spectra, the spectra collected were compared against

a common FTIR database (KnowItAll, Bio-Rad Inc.). The ~30 nm tall contamination residue was positively identified as polyethylene terephthalate (PET), a polymer typically used in polyester fabrics, as seen in Figure 2c.

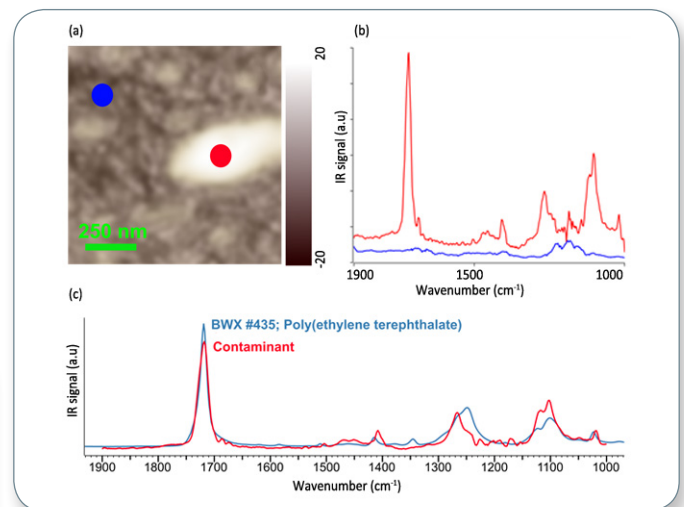


Figure 2. AFM height image (a) and resulting nanoIR spectra (b) from a contaminant on a bare silicon wafer. The resulting match from the FTIR library identifies the contaminant as Poly(ethylene terephthalate).

Process-Induced Defects²

Low- κ α -SiOC:H/Cu interconnects are a useful example of the susceptibility of contamination during manufacturing, due to the sensitivity low- κ α -SiOC:H exhibits in response to slight chemical modifications induced during fabrication. The structure of the interconnect device designed for this experiment is shown in Figure 3. The average width of the low- κ - α -SiOC:H varies from 1650 nm to 330 nm, well under the spatial resolution limits of conventional IR spectroscopy, testing the capabilities of nanoscale IR spectroscopy.

Figure 4a is an AFM topography image of the low- κ - α -SiOH/Cu structure. The markers on the image represent the locations for subsequent nanoIR measurements. Each nanoIR spectrum was collected

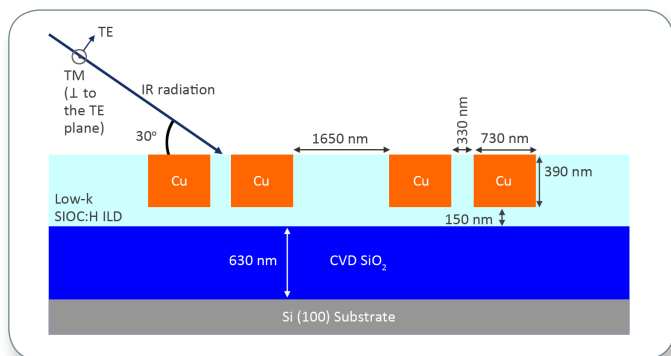


Figure 3. Schematic diagram of the cross section of the Low-K SiOC:H – copper interconnect structures fabricated for this experiment.

from a different portion of the interconnect, including both exposed regions of the α -SiOC:H dielectric, as well as copper. Spectra were also collected from narrow (390 nm) and wide (1650 nm) regions of the α -SiOC:H interconnect domains.

Close inspection of the spectra shown in Figure 4b reveals subtle differences in the C-H stretch region of the narrow and wide regions of the α -SiOC:H dielectric. The asymmetric methyl CH₃-stretching vibration at 2968 cm⁻¹ exhibited reduced intensity relative to the asymmetric methylene CH₂-stretching vibration at 2924 cm⁻¹ for the narrow regions of the α -SiOC:H dielectric. For the wide regions of the α -SiOC:H dielectric, the ratio of peak intensity for the CH₃/CH₂ modes was closer to that observed by both bulk FTIR and nanoIR of an unpatterned α -SiOC:H dielectric control sample, as seen in Figure 5.

To confirm that the differences observed in the C-H spectral regions of narrow versus wide α -SiOC:H regions aren't due to other phenomena, such as optical effects, spectra were also collected for the Si-O-Si stretching region.

Comparative differences were also observed in the nanoIR spectra of the Si-O-Si stretch from the wide versus narrow regions of the α -SiOC:H dielectric similar to the C-H stretch (Figure 5b). The primary observation is the relative difference in absorbance for the Si-O-Si cage mode at 1050 cm⁻¹, that is more prominent in the narrow regions of the α -SiOC:H dielectric relative to the wide regions. Relative to the bulk transmission FTIR spectra of the unpatterned α -SiOC:H dielectric, the cage mode for the 320 nm wide patterned α -SiOC:H region is also downshifted to lower, wavenumbers and the network Si-O-Si stretching mode appears to have a more narrow line width.

These combined results support the suggestion that the significant modification of the α -SiOC:H chemical structure occurs in the narrow regions of the α -SiOC:H/Cu interconnect structure relative to the wide regions. Numerous investigations of low- k - α -SiOC:H materials have shown a tendency for these materials to lose terminal methyl (CH₃) groups during the plasma etching,

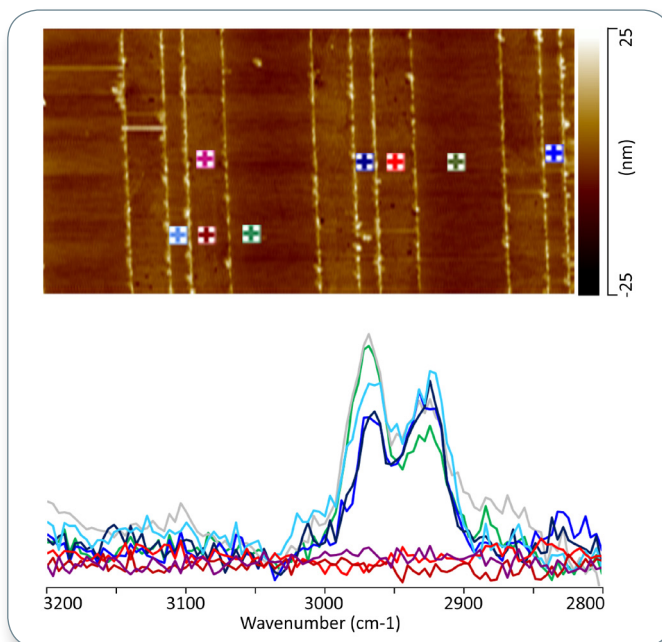


Figure 4. (a) 10 $\mu\text{m} \times 5 \mu\text{m}$ AFM topography image illustrating the regions from which the AFM-IR spectra were collected. Note the color of the marker corresponds to the color of the individual spectra. (b) AFM-IR C-H stretch spectra from the patterned α -SiOC:H/Cu interconnect.

ashing, and CMP steps utilized to fabricate inlaid Cu wiring. The loss of such terminal organic groups in low- k - α -SiOC:H dielectrics typically results in the formation of new chemical bonds and a more SiO₂-like composition.

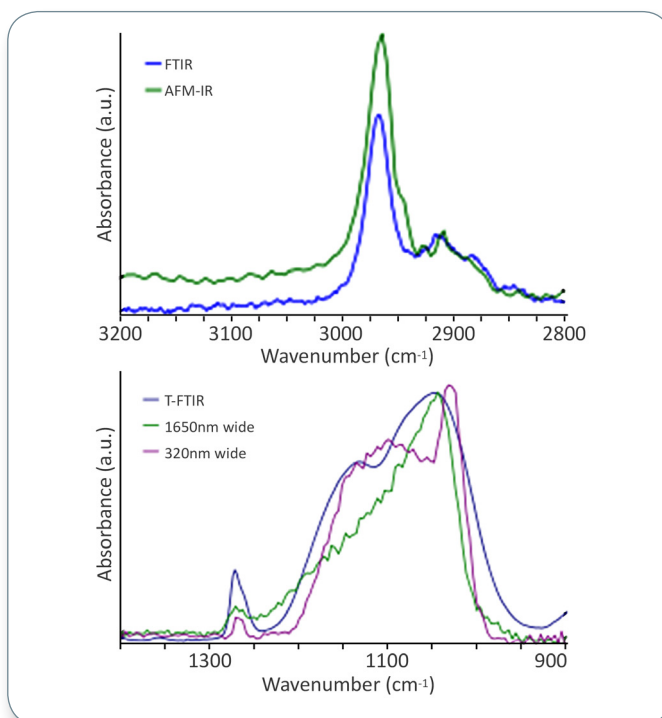


Figure 5. (a) T-FTIR and AFM-IR of the C-H stretching band from 1 μm α -SiOC:H. (b) spectra of the asymmetric Si-O-Si stretch and symmetric Si(CH₃)_x deformation mode from both narrow (390 nm) and wide (1,650 nm) regions of the α -SiOC:H dielectric. Note: a T-FTIR spectrum of the unpatterned α -SiOC:H dielectric is also included for comparison.

In this regard, the decrease in intensity of the CH₃ mode in the narrow regions of the α -SiOC:H dielectric, shown in Figure 4b, is consistent with the loss or modification of terminal CH₃ groups during the plasma etch and ashing processes utilized to pattern the dielectric. It is also consistent with the greater absorbance observed for the Si-O-Si cage mode in the narrow α -SiOC:H regions.

Characterizing Advanced Semiconductor Structures

For the last few decades, continuous development in semiconductor process technology has led to the fabrication of devices with ever shrinking nanometer scale domains. Directed self assembly (DSA) of block copolymers (BCPs), as shown in Figure 6, is one of the leading candidates for next-generation lithography providing sub-14 nm nanostructures with controlled placement.^{3, 4}

This breakthrough in nanoscale pattern fabrication using DSAs with 10-20 nm pitch results in a growing need for characterizing size, location, and alignment, as well as material-specific identification with high spatial resolution.

Recent developments in the AFM-IR technique, such as Tapping AFM-IR push the spatial resolution limit below 10 nm. Thus, this technique is ideal for chemically characterizing DSA components and defects for failure analysis (FA).⁵

In this experiment, Tapping AFM-IR was used to analyze different block copolymers routinely used to fabricate directed self-assemblies on Si wafers. Figure 7 demonstrates AFM topography and subsequent nanoscale chemical analysis of polystyrene-poly(2-Vinyl Pyridine) block copolymer [PS-P2VP]. The high-resolution topography image shows 3-4 nm tall lamellar features with 50 nm pitch. Subsequent chemical analysis with Tapping AFM-IR measurements explore the chemical compositions in the nanopattern. AFM-IR spectra directly correlate with FTIR absorption bands and highlight the distinct chemical signature of the components. Tapping AFM-IR imaging at absorption bands specific to each component, as shown in Figures 7(c), highlight the overall distribution, with an observed spatial resolution of 10 nm. The taller features were determined to be polystyrene blocks (domains) and the matrix P2VP.

Further measurements were performed on DSAs with different nanopatterns and functional molecules. Figure 8 shows chemical mapping of spherical DSAs consisting of both PS-*b*-PMMA and PS-*b*-P4VP [polystyrene-poly-4-vinylpyridine block copolymer]. The measurements yielded excellent chemical specificity with high spatial resolution, ~4 nm, as shown in the Figure 8 inset.

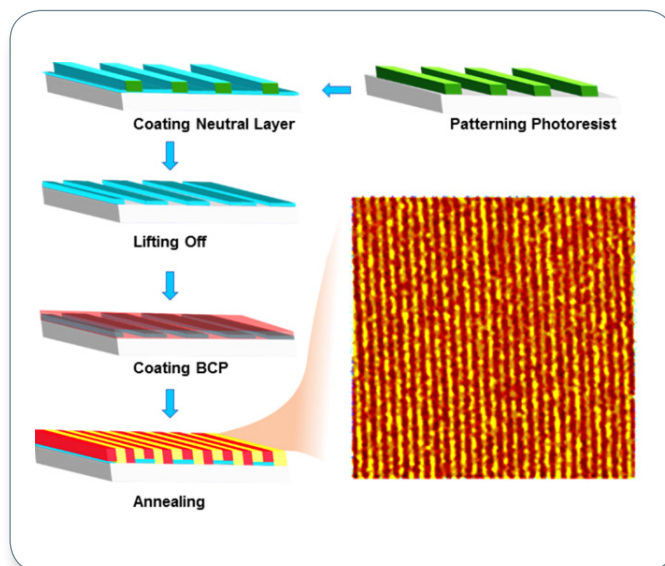


Figure 6. Illustrating 'lift-off' process to create epitaxial DSA patterns. The AFM image highlights the linear array of block copolymers.⁶

Conclusion

This application note demonstrates the successful application of Tapping AFM-IR to distinguish the chemical footprints of several nanoscale lithographic patterns consisting of complex molecular assemblies with excellent spatial resolution of 4 nm.

Additionally, nanoscale IR spectroscopy also excels in the characterization of nanoscale defects induced during low-k interconnect fabrication processes.

Significant chemical differences were observed for narrow

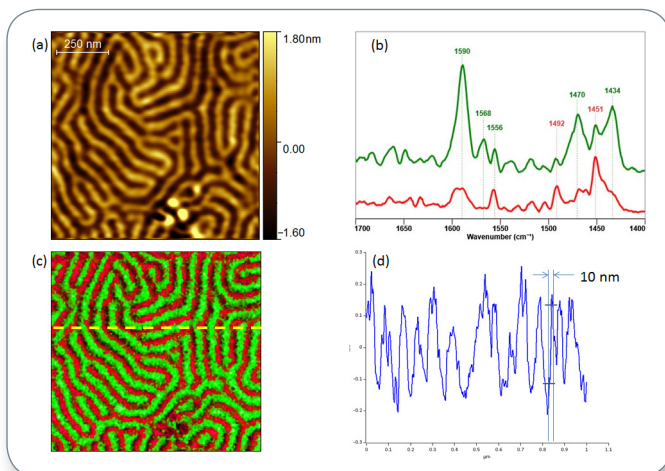


Figure 7. Chemical characterization of PS-P2VP block copolymer sample by Tapping AFM-IR; (a) Tapping AFM height image; (b) Tapping AFM-IR spectra clearly identifying each chemical component; (c) Tapping AFM-IR overlay image highlighting both components (PS@ 1492 and P2VP@ 1588); and (d) profile cross section highlighting the achievable spatial resolution, 10 nm. Sample courtesy of Dr. Gilles Pecastaings and Antoine Segolene at University of Bordeaux.

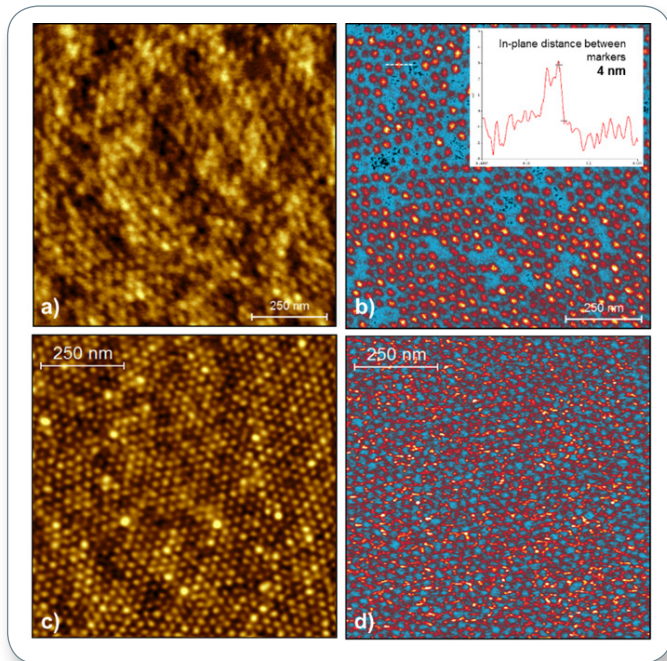


Figure 8. Tapping mode height images with PS-b-PMMA (a) and PS-b-P4VP directed self-assemblies (c). The nanopatterns are spherical with 10-20 nm domains. Tapping AFM-IR image at 1730 cm^{-1} highlights PMMA beads embedded in the polystyrene matrix (b). The ratio image at $1492\text{ cm}^{-1}/1598\text{ cm}^{-1}$ illustrate distribution of PS relative to P4VP in the patterned wafer (d). The inset in (b) shows the IR intensity variation along the white dashed line in the main panel. A spatial resolution of 4 nm is observed.

low-k regions when compared to thick regions. Due to the broad spectral range available for nanoIR, these differences were observed in both the Si-O-Si and CH stretching regions, where conventional IR spectroscopy cannot uncover these defects with its limited spatial resolution.

Finally, nanoIR spectra collected from common examples of nanoscale contamination were easily identified as biological material from the presence of the amide absorption bands; additionally, any spectra of unknown materials generated using nanoscale IR spectroscopy can be readily searched in a conventional FTIR database for easy identification.

It is clear from these results that nanoscale IR spectroscopy via AFM-IR shows great potential as a characterization tool for advanced semiconductor materials and processes.

Acknowledgements

The authors acknowledge Dr. Névine Rochat at University Grenoble Alpes, CEA-LETI and Dr. Gilles Pecastaings and Antoine Segolene at University of Bordeaux for block copolymer samples.

References

1. Dazzi, A. and Prater, C. B., "AFM-IR: Technology and Applications in Nanoscale Infrared Spectroscopy and Chemical Imaging", *Chem. Rev.*, 117 (2017), pp. 5146-5173.
2. Lo, M.; Dazzi, A.; Marcott, C.; and King, S., "Nanoscale Chemical-Mechanical Characterization of Nanoelectronic Low-k Dielectric/Cu Interconnects" *ECS Journal of Solid State Science and Technology* 2015, 5 (4), 3018-3024.
3. Yang, G. W. Wu, G. P. Chen, X. X. Xiong, S. S. Arges, C. G. Ji, S. X. Nealey, P. F. Lu, X. B. Darenbourg, D. J. and Xu, Z. K. "Directed Self-Assembly of Polystyrene-b-poly(propylene carbonate) on Chemical Patterns via Thermal Annealing for Next Generation Lithography", *Nano Lett.*, 17 (2017), pp. 1233-1239
4. Bates, F. S. and Fredrickson, G. H., "Block Copolymer Thermodynamics: Theory and Experiment", *Annu. Rev. Phys. Chem.*, 41 (1990), pp. 525-557
5. Roy, Anirban et al, ISTFA conference, "Latest Advancements in Nanoscale IR Spectroscopy for Characterization and Failure Analysis of Electronic Devices" 2017.
6. Figure modified from figure 3, Seong, S.J., et al., "Directed self-assembly of block copolymers for next generation nanolithography". doi10.1016/j.mattod.2013.11.002.